Supramolecular Repair of Hydration Lubrication Surfaces

Yixin Wang[#,1], Yulong Sun[#,1,2], Alyssa-Jennifer Avestro[2,3], Paul R. McGonigal[2,*], Hongyu Zhang[1,*]

[#] These authors contributed equally to this work

[1] State Key Laboratory of Tribology, Department of Mechanical Engineering, Tsinghua University, Beijing 100084, China
Tel: +86 010 62796053
Fax: +86 010 62781379

Email: zhanghyu@tsinghua.edu.cn

[2] Department of Chemistry, Durham University, Lower Mountjoy, Durham, DH1 3LE, UK
Tel: +44 191 334 2593

Email: paul.mcgonigal@durham.ac.uk

[3] Department of Chemistry, University of York, Heslington, York, YO10 5DD, UK
Tel: +44 190 432 8962

[*]Correspondence to Dr Paul R. McGonigal and Dr Hongyu Zhang

SUMMARY

Although advances in coating technologies have allowed us to match—or even exceed—the lubricity of Nature's low-friction surfaces, the performance of synthetic materials inevitably diminish over time as the surfaces are worn and damaged by irreversible breakage of covalent bonds. Synthetic systems lack the bespoke repair mechanisms that replenish hydration lubrication surfaces in Nature. Here, we demonstrate dynamic repair of low-friction surfaces prepared through a surface-selective self-assembly strategy. Monolayers of lubricating polymers associate with functionalized surfaces through strong and specific host–guest interactions, leading to hydration lubrication surfaces with low coefficients of friction (0.024–0.028). Following friction-induced dissociation of the polymers, the polymer-to-surface interaction is restored by the reformation of host–guest complexes, thus repairing the monolayer, renewing the surface lubricity, and reducing the effects of wear. Such dynamically restored low-friction materials will be an essential tool in decreasing global energy use – a fifth of which is expended overcoming friction.

RESULTS AND DISCUSSION

Low-friction materials that have evolved in Nature, such as the articulating cartilage surfaces found in healthy human joints,[1,2] exhibit remarkably low coefficients of friction (COFs). In many cases, they attain their low COFs as a result of hydration lubrication.[3,4] Layers of water molecules, which are tightly bound to the lubricating surfaces, relax rapidly when subjected to shear, minimizing drag and giving COFs down to 0.001.[3] Synthetic low-friction materials that draw inspiration from the high-lubricity surfaces in Nature have become central to the investigation of fundamental interfacial phenomena and to technological applications, where their low sliding resistance and minimal wear limit energy waste and prevent premature mechanical failure.[1,5]

Beyond lubricity, ideal low-friction surfaces should also possess (i) sufficient malleability to dissipate compressive stress,[6] (ii) high resistance to mechanical wear and surface degradation over extended periods of shear and repeated impact events, as well as (iii) a simple means of repair for when degradation inevitably occurs by the breakage (Figure 1a) of covalent bonds. Robust low-friction materials, such as poly(tetrafluoroethylene) (i.e., Teflon®), graphene,[7] and diamond-like carbon,[8] are available but have inherently high stiffnesses, which hinders their use in articulating materials and at
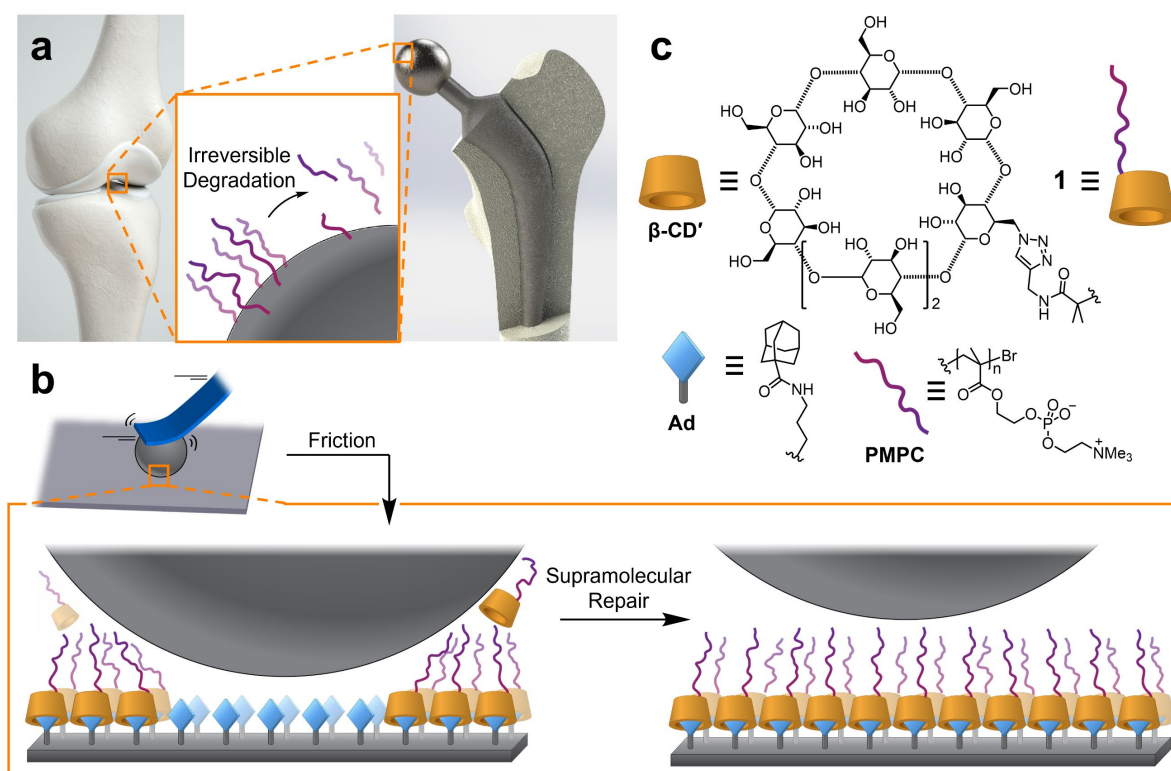
Figure 1 Illustration of the differences between irreversible wear of a covalently functionalized surface and dynamic repair of a reversibly assembled lubricating layer. **a** Natural cartilage and artificial hip joints can be lubricated by covalently attached (bio)polymer layers, which undergo irreversible mechanical wear through breakage of covalent bonds, whereas **b** a surface-bound layer of lubricating β-CD′-PMPC polymer, **1**, is restored upon reforming noncovalent bonds with surface-bound Ad units after friction-induced dissociation. An idealised monolayer is shown for simplicity. A mixture of vacant sites, mushroom-like and brush-like polymer domains are likely present at equilibrium. **c** Structural formulas of the components of the hydration lubrication surface. Ad is connected to a Ti surface through a silane linkage.[13]

soft interfaces.[9] Soft, easily reparable, low-friction surface coatings are needed in the context of, for example, artificial hip joints,[10–12] whose wear over time (Figure 1a) can lead to complications requiring further medical treatment. In recent years, therefore, research has been directed towards soft surface coatings that meet criteria (i)–(iii).

Compressible hydration lubrication surface coatings have been prepared from a variety of synthetic materials—surfaces have been coated with non-specific adsorbents, such as liquid surfactants[3] and bio-mimetic lipid bilayers,[14] or covalently functionalized with (super)hydrophilic polymer brushes.[9,15,16] Zwitterionic poly(2-methacryloyl-oxyethyl phosphorylcholine) (PMPC) materials[9] perform particularly well, recruiting the layer of water molecules needed to enact hydration lubrication and achieving record-low (<0.001)[3,17] COFs in certain cases. Yet, state-of-the-art hydration lubrication surfaces and other biocompatible low-friction materials currently lack robustness or an ability to repair dynamically in a prescribed manner. Indeed, self-healing boundary lubricants have been developed based on immiscible fluid layers immobilised on porous surfaces,[18] ionogels,[19] and microcapsule-impregnated polymers.[20] However, in general, there has been a dichotomy between high wear resistance and flexibility, while limited progress has been made[21] towards simple surface repair mechanisms that could operate in biologically relevant settings. Progress is needed in this area to minimise the irreversible degradation of covalently bound surface layers that inevitably occurs (Figure 1a) when surfaces are subject to repeated wear.

Here, we report the design, synthesis, and investigation of dynamically repairing hydration lubrication surfaces based on the self-assembly of polymer monolayers through strong and specific host–guest interactions that operate in water. When friction is applied to the surfaces, the host–guest complexes, which serve as pre-programmed weak links, dissociate preferentially. We show that surfaces can recover from mechanical wear by reformation of the noncovalent bonding interactions, which in turn restores lubricity.

Molecular Design and Synthesis

We sought to develop a strategy for incorporating a low-friction coating onto surfaces by taking advantage of the dynamic reversibility and specificity of host–guest interactions. We hypothesized that such interactions between a guest-decorated surface and a host-functionalized lubricating polymer would enable the surface to recover from damage (Figure 1b) through reversible supramolecular assembly, which would be helpful in circumventing the effects of mechanical wear. The biocompatible and bioorthogonal[22,23] interaction of macrocyclic β-cyclodextrin (β-CD) hosts with adamantyl guests[24–26] has been successfully applied to generate self-healing hydrogels,[27–31] to prepare self-assembled monolayers,[32–35] and to organise polymers on the surface of vesicles.[36] Adamantyl guests are well matched to the hydrophobic cavity of β-CD, typically giving rise to high association constants, K_a, of ~3×10^4 M^{-1} in aqueous solution.[24] Therefore, compound **1** was identified (Figure 1c) as a suitable target. It incorporates a β-CD macrocycle derivative (β-CD′) at the terminus of a PMPC backbone, enabling highly selective interactions with surface-bound 1-adamantane carboxamide (Ad)

residues.

We prepared **1** in two steps from propargyl 2-bromo-2-methylpropionamide (BMP). In the first step, a 2-methacryloyloxyethyl phosphorylcholine (MPC) monomer was subjected to atom-transfer radical polymerisation (ATRP) conditions using BMP as the initiator, which afforded an alkyne-terminated polymer. See the Methods section and Supplementary Information for detailed procedures. A Cu(I)-catalysed azide–alkyne cycloaddition (CuAAC) reaction with mono-(6-azido-6-deoxy)-β-cyclodextrin was used to link the terminus of the polymer to the primary rim of β-CD′, giving **1**. We also prepared a fluorescein-tagged analogue, **1′**, by copolymerizing a 1:14 ratio of fluorescein *O*-methacrylate monomer with MPC before subjecting the resulting alkyne to the same CuAAC conditions. Both lubricating polymers **1** and **1′** have been structurally characterized by Fourier transform infrared (FTIR), fluorescence, and nuclear magnetic resonance (NMR) spectroscopies, as well as size-exclusion chromatography (SEC). See the Supplementary Information. The SEC data (Table S3) reveals a multimodal distribution of polymers **1** and **1′** in which the major components possess molecular weights of 297 and 59.1 kDa, respectively. The polydispersities measured (1.3 – 1.6) are a consequence of the mixed solubility profiles of the charged intermediates produced during polymerisation.

Surface Functionalization

In order to probe the lubricating and dynamic self-assembly properties of **1**, we functionalized the surface of Ti-6Al-4V (Ti) wafers with Ad groups that complement the β-CD′ end group of the PMPC. Firstly, alkylamine-functionalized substrates, **Ti-NH₂**, were prepared by treating Ti wafers with aminopropyltriethoxysilane (APTES).[13] We verified the presence of primary alkylamino groups on the surfaces by performing (Figure 2) attenuated total reflection (ATR) FTIR analysis and X-ray photoelectron spectroscopy (XPS), observing (i) absorbances at 3352 and 3282 cm⁻¹ that arise (Figure 2a) from symmetrical and asymmetrical stretching vibrations of NH₂ groups[37] and (ii) photoelectrons in the N1s region with a binding energy of 398 eV, indicative (Figure 2b) of a single N-atom environment. The **Ti-NH₂** wafers were further functionalized by treating with 1-adamantanecarboxylic acid chloride in order to covalently connect (Figure 1c) Ad residues to the surfaces. XPS analysis of the resulting **Ti-Ad** substrates shows that a significant proportion of the **Ti-NH₂** reactive sites are converted to Ad groups. Peak fitting of the C1s region of the **Ti-Ad** spectrum reveals (Figure 2b) the emergence of a shoulder at ~288 eV, which matches the binding energy expected for an amide C environment[38] and has low intensity in keeping with its low abundance relative to alkyl C atoms. Two signals can be distinguished at 398 and 400 eV in the N1s region, which suggest the presence of N atoms in two bonding environments. The N and C signals are consistent, therefore, with a mixture of adamantane carboxamide linkages and unreacted amine groups being present on the surface. The signal at 398 eV, which we assign as the primary amine by comparison with XPS of **Ti-NH₂**, accounts for 67% of the peak area, indicating an amine–amide ratio of 2:1.

The lubricating surface layer was assembled by submerging a **Ti-Ad** wafer in a 10 mg/mL aqueous
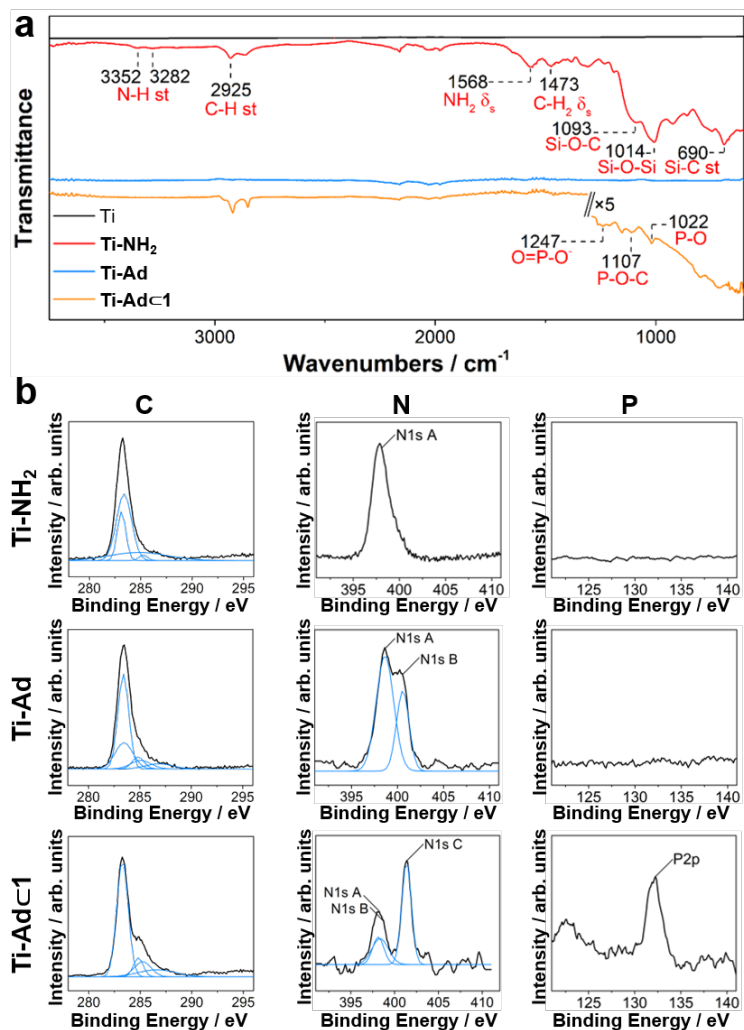
Figure 2 Characterization of functionalized **Ti-NH₂**, **Ti-Ad**, and **Ti-Ad⊂1** wafers. **a** ATR-FTIR spectra, **b** X-ray photoelectron spectra with peak-fitting traces shown in blue. FTIR signals of **Ti-Ad⊂1** below 1300 cm⁻¹ are magnified by a factor of 5.

solution of **1** at room temperature. Under these conditions, the self-assembling system reaches equilibrium over approximately two hours (vide infra). We immersed the wafer in the solution of **1** for 12 hours to ensure the surface coating had fully equilibrated. After removing the wafer from the solution, it was rinsed with deionized water and the surface was analysed to detect the surface-bound polymer. The ATR-FTIR spectrum of this wafer, **Ti-Ad⊂1**, exhibits (Figure 2a) absorbances typical of phosphate groups in the 1000–1250 cm⁻¹ region of the infrared spectrum and XPS analysis shows (Figure 2b) additional signals in the N1s and P2p regions, as would be expected for a surface coated with the phosphorylcholine groups of **1**. The P signal at 132 eV appears as an asymmetric peak as a consequence of its overlapping P2p3/2 and P2p1/2 components, which is typical for phosphates.[38] These measurements show, therefore, that the **Ti-Ad⊂1** wafer retains adsorbed **1** after rinsing with water as a result of the noncovalent bonding interactions between the polymer and the surface. Assembly of **1** on a similarly functionalised **Ti-Ad** surface of a quartz crystal microbalance (QCM) sensor was also measured, revealing (Supplementary Table S5) a surface coverage of 1.8 pmol·cm⁻¹ that is consistent with a mushroom-like surface monolayer of adsorbed polymer.

Friction Properties

We investigated the nanotribological properties of the surfaces under ambient conditions. First, we used atomic force microscopy (AFM) to measure (Supplementary Figure S18) the adhesion forces between a β-CD-modified polystyrene-microsphere AFM tip (see Supplementary Information for the preparation procedure) and the Ti surfaces immersed in water.[39] While the **Ti-Ad⊂1** substrate and an unmodified Ti substrate exhibit similar adhesive forces (37 and 49 nN, respectively) when brought into contact with the β-CD-coated tip, the **Ti-Ad** substrate experiences a significantly larger adhesive force of 262 nN. We attribute this difference to the strong and specific noncovalent bonding interactions that develop between the macrocyclic hosts of the tip and the free Ad guests of the **Ti-Ad** surface.[40,41] The apparent lack of these interactions between the AFM tip and the **Ti-Ad⊂1** surface suggest that the Ad groups of **Ti-Ad⊂1** are largely occupied, rendering them essentially unavailable to bind the β-CD macrocycles of the AFM tip. This observation illustrates the selectivity of the assembly process – a surface lacking free Ad groups does not interact strongly with the end groups present in polymer **1**.

Next, using a 5 μm-diameter polystyrene microsphere AFM tip coated with PMPC[42] (Figure 3, inset), we carried out friction force measurements with alternant loads of 400 and 500 nN applied (Figure 3) to the surfaces, giving contact pressures >54 MPa to simulate the pressures experienced by hip joints during exercise.[43] Microscopic friction forces were measured by scanning the PMPC-coated AFM tip at a frequency of 2 Hz across a sliding area of 20 × 20 μm for 2 minutes while the surfaces were immersed in either pure water or a 10 mg/mL aqueous solution of **1**. This concentration optimises
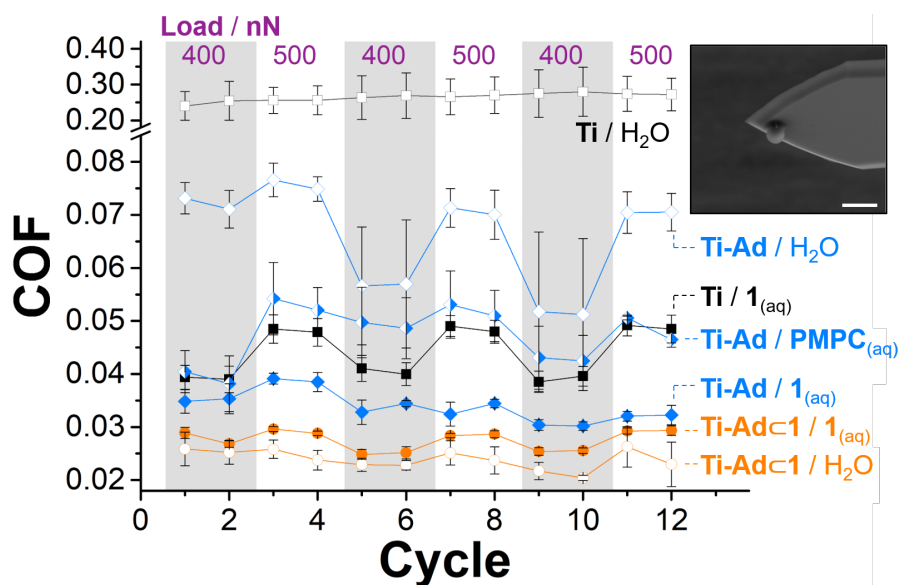
Figure 3 Friction force performances measured by AFM in contact mode show that the optimum COF is obtained when all components of the self-assembling system are present. The COF is derived by dividing the lateral force observed by the normal force applied. Measurements were performed on surfaces immersed in either pure H_2O, represented by hollow data points, a solution of PMPC in H_2O (10 mg/mL), shown by half-filled data points, or a solution of **1** in H_2O (10 mg/mL), shown with filled data points. The gray and white areas of the plot correspond to cycles performed using AFM-tip normal forces of 400 nN and 500 nN, respectively. Error bars show the standard deviation over three samples. **Inset**. SEM image of the PMPC-coated polystyrene-microsphere AFM tip. Scale bar = 10 μm.

performance without exceeding the solubility limit of the polymer (Table S4). Literature COF values for two interacting PMPC-coated surfaces in water – where each surface is covalently functionalized with a polymer monolayer – are typically in the range of 0.01–0.05 on account of efficient hydration lubrication,[44–46] and can be extended to as low as 0.001 for highly optimized systems.[3,4] In our investigation, the largest friction forces were measured (Figure 3) when the PMPC-coated AFM tip was applied to an unmodified Ti surface in pure water, giving rise to a COF of 0.264. Employing an aqueous 10 mg/mL solution of **1** as the medium reduces the COF fivefold to 0.044 by virtue of the additional hydration lubrication provided by weakly adsorbed polymer molecules on the Ti surface and polymer present in the medium immediately surrounding the contacting surfaces.[3] Covalent modification of the Ti surface with primary amine and Ad residues also reduces friction—although it does so to a lesser extent. The **Ti-Ad** substrate exhibits a COF of 0.067 in pure water. Exposing the **Ti-Ad** substrate to a 10 mg/mL aqueous solution of PMPC lacking a β-CD head group lowers the COF slightly to 0.047 on account of non-selective adsorption of the polymer to the Ad surface. Importantly, however, we observe the lowest COF values for our substrates when all components of the host–guest system are present. A **Ti-Ad** wafer freshly immersed in the solution of **1** exhibits a COF of 0.034—a twofold improvement relative to the COF measured for the same surface in the absence of the host-functionalized polymer. The COF is further improved to 0.024–0.028 when a pre-complexed substrate, **Ti-Ad⊂1**, is used (Figure 3) in place of the **Ti-Ad** wafer in either H_2O or the solution of **1**, suggesting that the lubricity of the surface increases when the self-assembly of the surface layer has fully equilibrated. Indeed, the lubricities of the equilibrated **Ti-Ad⊂1** substrate measured (Figure 3) in H_2O and **1**$_{(aq)}$ are similar to one another, which is consistent with the surface-bound layer of **1** present on the **Ti-Ad⊂1** substrate resisting dissociation even when the surface is immersed in H_2O. The selectivity of the noncovalent bonding interactions is evident when comparing the performance of the bare Ti and **Ti-Ad** substrates in the presence of **1**, where the guest-functionalised surface exhibits a significantly lower COF. Overall, the nanotribological experiments demonstrate that favourable host–guest interactions between the β-CD′ and Ad groups lead to a surface coating of phosphorylcholine groups being recruited by the Ti surface, which enacts hydration lubrication and reduces the overall drag experienced when the surface is rubbed.

Supramolecular Repair of the Lubricating Surfaces

In order to investigate the ability of the self-assembled surface to be dynamically repaired when subjected to mechanical wear, we prepared two coated glass slides, labelled **Glass-Ad⊂1** and **Glass-Ad⊂1′**, suitable for confocal laser scanning microscopy (CLSM) analysis. The slides were fabricated following procedures similar to those described for the preparation of the **Ti-Ad⊂1** substrates – functionalized **Glass-Ad** slides were prepared by covalent bond formation and then subjected to self-assembly conditions with either polymer **1**, to give **Glass-Ad⊂1**, or fluorescently labelled analogue **1′**, giving **Glass-Ad⊂1′** (see Supplementary Information). The successful modification of the glass substrates is evident (Figure 4) by the uniform green emission visible from the **Glass-Ad⊂1′** surface by CLSM while irradiating with 485 nm laser light to excite the fluorescein chromophores of polymer

1′, as well as XPS analysis (Figure S17). We subjected this **Glass-Ad⊂1′** substrate to mechanical wear by AFM while under a 10 mg/mL aqueous solution of non-emissive **1**, applying a 400 nN normal force through a bare polystyrene-microsphere tip in contact mode as it was repeatedly scanned across a 20 × 20 μm area at 2 Hz for 20 minutes. A bare polystyrene-microsphere tip was used to maximize wear – similar experiments performed with PMPC-coated tips did not cause a noticeable change in the surfaces over the course of the 20-minute experiments. After wearing the **Glass-Ad⊂1′** slide with the bare polystyrene-microsphere tip, it was allowed to stand in the solution of **1** for two hours. CLSM analysis of the surface shows (Figure 4a) that the worn area becomes non-emissive, which suggests that the fluorescent polymer **1′** has desorbed from the surface, being replaced by **1**. The reformation of β-CD′–Ad interactions restores the lubricating monolayer (vide infra). To better visualize the repair step and confirm that the surface is indeed repaired by assembly of polymer from solution, we conducted the converse experiment using a non-emissive **Glass-Ad⊂1** substrate immersed in a solution of the fluorescent polymer **1′**. Initially, the surface is non-emissive, but the worn area becomes fluorescent (Figure 4b) upon exchange of surface-bound **1** for **1′** from solution. The areas of the glass slide that have not been worn remain relatively non-emissive, illustrating that the desorption is accelerated (Figure S24) by the mechanical wearing process. Taken together, the exchange processes observed on **Glass-Ad⊂1** and **Glass-Ad⊂1′** substrates demonstrate that (i) in the absence of friction,
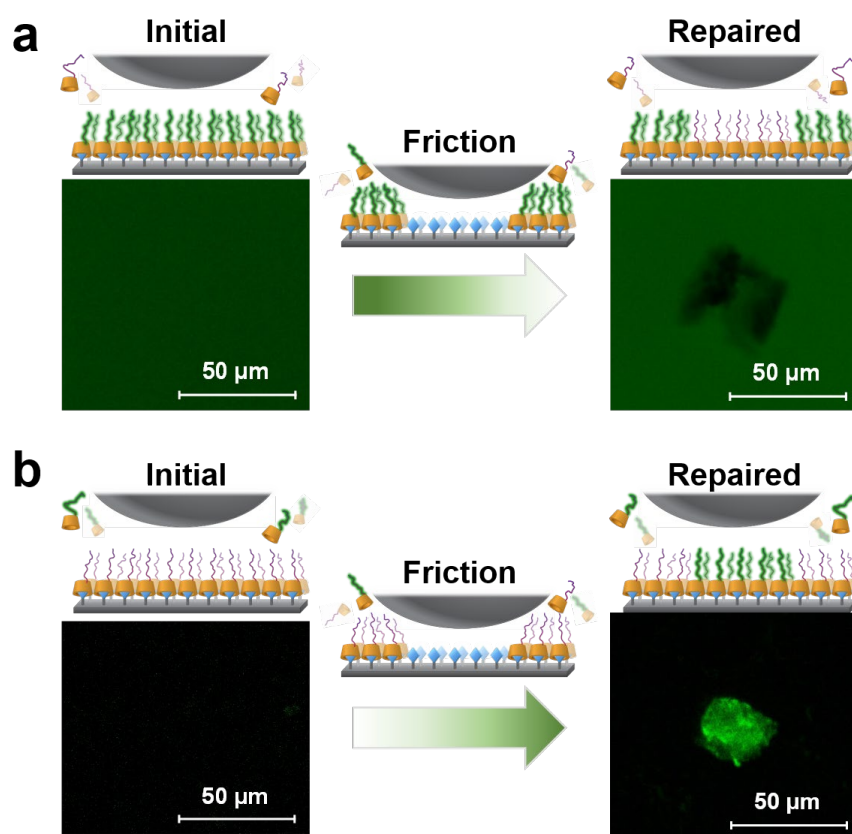
Figure 4 Confocal laser scanning microscope images of ~20 × 20 μm worn areas created by applying 400 nN normal force in AFM contact mode (polystyrene-microsphere tip) across glass slides. **a Glass-Ad⊂1′** under a 10 mg/mL aqueous solution of **1** and **b Glass-Ad⊂1** under a 10 mg/mL aqueous solution of **1′**. An idealised monolayer structure is depicted for simplicity. Under the experimental conditions, worn areas will equilibrate (i.e., self-heal) to replicate the mixture of vacant sites, mushroom-like and brush-like polymer domains.

the initially adsorbed polymer layer is metastable, desorbing partially over a 12-hour period (Figure S24). There are not significant amounts of background desorption while the surfaces are immersed in solution over the two-hour timescale of the experiment, even in the presence of a competitive host molecule in the solvent medium. This observation is consistent with strong and selective interactions between the CD groups of **1** and the Ad-functionalized surface rather than weak, non-selective binding. Previously, Huskens et al. have observed similar metastability of densely packed monolayers formed by interactions of β-CD and multivalent Ad guests.[32,33] Our experiments also reveal that (ii) the 400 nN normal force, which corresponds to a shear stress of 7.5 MPa at the COF for this surface of 0.138 (Figure 5) with the bare polystyrene-microsphere AFM tip, is sufficient to cause the noncovalently attached polymers to desorb from the surface, but (iii) does not significantly degrade the covalently bonded Ad sites of the modified glass substrates. As a result, (iv) the surface is dynamically repaired by self-assembly of a fresh layer of lubricating polymer from the bulk solution as the favourable β-CD′–Ad interactions reform.

Finally, we investigated (Figure 5) whether repair of the self-assembled polymer layers also restores the lubricity of the surfaces. We wore a 20 × 20 μm patch of **Glass-Ad⊂1** substrate under pure water using a bare polystyrene-microsphere AFM tip with a normal force of 500 nN at 2 Hz for 30 minutes, ensuring that a significant quantity of the polymer would desorb. In the absence of dissolved polymer, the surface layer would not be expected to repair. Indeed, we observed that the COF between the substrate and bare polystyrene-microsphere AFM tip increased from an initial value of 0.138 for the self-assembled surface to 0.533 after being worn. The worn area was then immersed in a 10 mg/mL aqueous solution of **1** while intermittently performing friction force measurements under a normal force of 400 nN to monitor (Figure 5a) the change in COF over time as the surface is repaired. We observed that the lubricity is gradually restored on the minute-to-hour timescale, plateauing after approximately two hours. This dynamic restoration of the **Glass-Ad⊂1** substrate returns the COF (Figure 5b) to 0.208.

The kinetics of the repair process are consistent with the kinetics of association observed by QCM (Figure 5c,d) and with the observed resistance of the fully equilibrated polymer layers to desorption[47] under ambient conditions, e.g., when the solvent medium is exchanged (Figure 4). The QCM measurements indicate that when a **Ti-Ad** surface is first exposed to **1**(aq), the surface is rapidly coated with an initial layer of the polymer, reaching two thirds of the eventual surface-bound polymer mass within 2 minutes. However, the mass of adsorbed polymer continues to increase gradually over a period longer than 30 minutes as the self-assembled monolayer equilibrates towards a more closely packed structure. Comparison with the lubricity over a similar period indicates (Figure 5a) that this closely packed PMPC layer is needed to impart a low COF.
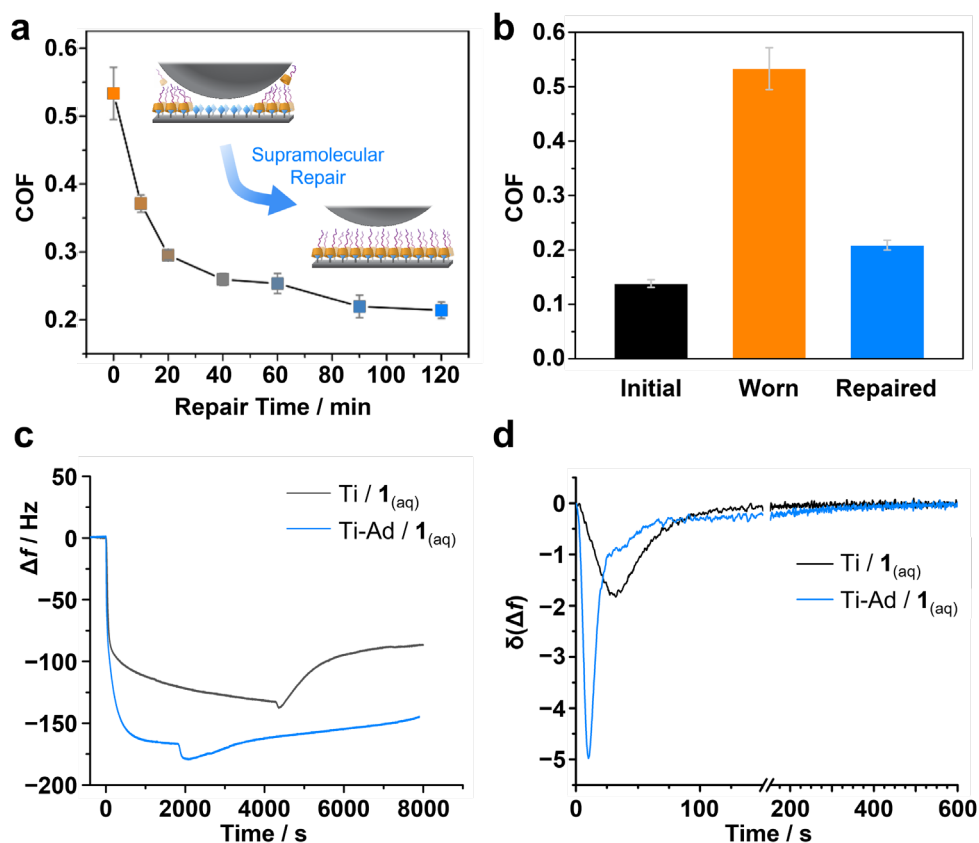
Figure 5 Supramolecular repair of the hydration lubrication polymer surface after wear-induced polymer desorption restores the COF to near its initial value. The COF was measured using a normal force of 400 nN applied through a bare polystyrene-microsphere tip. **a** The COF of the worn area of a **Glass-Ad⊂1** slide decreases over time as it stands in a 10 mg/mL aqueous solution of **1**. **b** Comparison of the COF before the surface is worn, after wearing in pure water for 20 min under a 500 nN normal force, and after subsequent healing in a solution of **1** for 2 h. Bars: standard deviation over three trials. **c** QCM data showing adsorption of 10.0 mg/mL aqueous **1** on a chip with either a bare Ti surface or a **Ti-Ad** surface for the n = 3 overtone. Sample injection occurs after an initial equilibration with H_2O (set as t = 0 s) and proceeds at a flow rate of 100 μL·min^{-1} until a plateau in frequency is reached, before switching back to H_2O. The runs were performed up to a total of 8000 s (~2.25 h). The changes in frequency immediately before switching back to H_2O (i.e., at the end of adsorption), $\Delta f_{solution}$, and at the end of the 8000 s run after the rinsing period, Δf_{rinsed}, were used to calculate the mass densities shown in Supplementary Table S5. **d** Differentials of the data from part **c**, showing that **1** adsorbs to the **Ti-Ad** surface at a higher initial rate than to the bare Ti surface, but that the bare Ti surface reaches a plateau in frequency more quickly.

Conclusions

A diverse set of technologies stand to benefit from improved low-friction materials, ranging from artificial biomedical implants[7–9] and micro- or nanoelectromechanical systems,[48] to energy-efficient vehicles[49]. While optimization of absolute surface lubricity is clearly a primary consideration, the longevity of materials is also of paramount importance. Materials must perform over repeated cycles of operation, either by resisting degradation when subjected to mechanical wear or by employing mechanisms that replenish lubricating surface coatings. Nature's lubricating surfaces, such as the cartilage found in human joints, are replenished by biological machinery that reconstructs the covalent structures of self-assembling surface layers. We have demonstrated that a phenomenologically different repair strategy can achieve a similar effect in synthetic materials, making use of simple

molecular components—self-assembled surface coatings of lubricating polymers combat degradation by dynamic restoration of the surface structure, reversing the effects of mechanical wear and restoring lubricity. We have exemplified this concept using the noncovalent bonding interactions between a functionalized β-CD′ polymer and Ad groups in water. The self-assembly recruits a lubricating layer of PMPC to the surface, which friction force measurements have shown to perform similarly to other PMPC-based hydration lubrication systems. By contrasting the behaviour of a fluorescently-tagged polymer with the non-emissive analogue and performing friction force measurements, we have shown that the self-assembled system undergoes exchange when worn. Mechanical wear breaks the noncovalent bonding interactions, which, on account of their inherent reversibility, then re-establish dynamically to repair the surface and restore lubricity. Though they are not as low as the most highly optimised covalent-link systems reported (0.001),[3,4] the COF values obtained by our weak-link supramolecular concept (0.024–0.028) are characteristic[44–46] and well within the range of established hydration lubrication systems (0.01–0.05). Unlike these established systems, our results demonstrate that the specificity of supramolecular host–guest interactions can be exploited to assemble a low-COF hydration lubrication layer that is simultaneously capable of dynamic repair. Future optimisation and tuning of weak-link host–guest pairs will be required to match the lubricity of purely covalent surface coatings. In this proof-of-concept system, the self-assembled surface monolayer is remarkably resistant to desorption, exhibiting metastability on the timescale of several hours while submerged in water despite its assembly being driven by discrete, monovalent β-CD′–Ad interactions. The application of multivalent[35,50] surface-to-polymer interactions may further enhance the stability of the surface coating while allowing the friction-induced breakage and subsequent reformation of noncovalent bonding interactions to occur without complete dissociation. The biocompatibility and biorthogonaliity[22,23] of the components bode well for the application of this, or similar, surface-selective self-assembly systems in the context of artificial joint lubrication to extend the lifetimes of medical implants. By analogy to synthetic polymers that can be injected into synovial joints to treat osteoarthritis,[21] solutions of polymers exhibiting selective noncovalent bonding interactions with artificial joints could be employed to restore their hydration lubrication surfaces, mitigating the effects of enzymatic and friction-induced degradation. This selective self-assembly strategy may also be of broader applicability as part of more durable low-friction materials, which are needed to increase the energy efficiency of mechanical devices in general.

Materials and Methods

MPC was supplied by *Joy-Nature Corp. (Nanjing, China)*. APTES, anhydrous toluene, propargylamine, trimethylamine, 2-bromopropionyl bromide, CuBr, CuI, *N,N,N′,N′′,N′′*-pentamethyldiethylenetriamine (PMDETA) and *tert*-butyl hydroperoxide were purchased from *J&K Scientific Ltd. (Beijing, China)*. Amine-modified polystyrene microspheres (4.0–4.9 µm diameters) were purchased from *Aladding Corp. (Shanghai, China)*. The 'TL-CONT' variety of tipless AFM cantilever probe was purchased from *NanoWorld AG (Geneva, Switzerland)*. Ti wafer (10 × 10 mm, Ti-6Al-4V) was purchased from *Goodfellow Inc. (London, England)*. Petroleum ether, ethanol, acetone, tetrahydrofuran (THF) and *N,N*-dimethylformamide (DMF) were purchased from *Modern Oriental Technology Development Co., Ltd. (Beijing, China)*.

NMR spectra were recorded by using an Ascend 400 MHz spectrometer or Ascend 800 MHz spectrometer from *Bruker Co. Ltd., Billerica, USA*. ATR-FTIR spectra were recorded by using a Nicolet FTIR 6700 instrument (*Thermo Fisher Scientific Inc. Waltham, USA*) fitted with an ATR module. XPS data were recorded using an X-ray photoelectron spectrometer (*PHI Quantera II, Bruker, Billerica, USA*) equipped with a 15 kV Mg-Kα radiation source. The take-off angle of the photoelectrons was maintained at 90°, and five scans were taken for each sample. Friction experiments were accomplished by using an MFP-3D Classic atomic force microscope *from Oxford Instruments Asylum Research, Inc. Santa Barbara, CA, USA*.

Friction Performance Measurements

Normal and friction force measurements were performed on the *Asylum Research* MFP-3D AFM in contact mode. The spring constant of the TL-CONT probe was determined by the frequency method,[51] and the lateral sensitivity of the probe was obtained by the improved wedge calibration method before the measurement.[52,53] The friction tests were performed at room temperature, over a sliding area of 20 × 20 μm, at a sliding angle of 90°, and frequency of 2 Hz, using a PMPC-coated AFM tip (see below for preparation details). In order to simulate the pressure that hip joint undergo during strenuous exercise[48], we choose two different normal forces under which the pressure of contact area exceeds the actual contact pressure[54] in natural hip joint, i.e., 2.6 MPa (see Supplementary Information). Either pure water or a 10 mg/mL aqueous solution of **1** were used as the lubricant. During the test, three random areas of 20 × 20 μm were chosen to carry out friction tests in each group. Each area was subjected to three successive cycles of normal force through stages of two scans each at 400 nN then 500 nN. Each normal force in the cycles was applied to scan the whole 20 × 20 μm area once in 128 seconds (256 lines per area and scan rate of 2 Hz).

Surface-Repair Experiments

Dynamic repair properties were characterized by applying a friction force to a substrate by AFM using a bare polystyrene microsphere AFM tip, then examining the surface using CLSM. In order to observe wear area by CLSM, we used coated glass slides that were prepared by the same method used to functionalize the Ti-6Al-4V wafers (see Supplementary Information). During the friction experiments, **Glass-Ad⊂1** was worn under the normal force of 500 nN of a colloidal polystyrene AFM tip for 30 min, then 200 μL of 10 mg/mL **1**$_{(aq)}$ solution was added onto the slide to allow the worn area to repair. The COF of the worn area was measured at regular intervals by AFM (normal force: 400 nN, sliding distance: 20 μm, scan area: 20 × 20 μm, scan rate: 2 Hz). To visualize the polymer desorption and subsequent restoration, a **Glass-Ad⊂1′** slide was worn under 10 mg/mL of **1**$_{(aq)}$ solution and **Glass-Ad⊂1** was worn under 10 mg/mL of **1′**$_{(aq)}$ solution. The slides were worn at room temperature under the same experimental conditions as before (wearing under a normal force of 500 nN using a bare polystyrene microsphere AFM tip for 30 min).

Preparation of Ti-Ad Wafers

The surfaces of commercially sourced Ti-6Al-4V wafers were firstly cleaned by ultrasonication in pure water and acetone for 5 min and dried under nitrogen flow. Then the cleaned wafers were functionalized with amine groups by silanization of the Ti surface using APTES. Adamantane groups were then grafted onto the surfaces by acylation of the amines with 1-adamantanecarboxylic acid chloride. For specific experimental details, see the Supplementary Information (Scheme S6).

Synthesis of 1 and 1′

1 was prepared by a three-step method shown in Schemes S1, S2 and S4 of the Supplementary Information. Briefly, BMP was synthesized by amidation of 2-bromopropionyl bromide with propargyl amine (Scheme S1) then used as an initiator

to synthesize an alkynyl-terminated-PMPC polymer (alkynyl-PMPC) through ATRP (Scheme S2) of MPC. The alkynyl-PMPC was modified via a CuAAC reaction with mono-(6-azido-6-deoxy)-β-cyclodextrin (Scheme S4), yielding **1**. The fluorescein-copolymer analogue **1′** was prepared by the same synthetic route (Schemes S3 and S5), adding a small amount of fluorescein-*O*-methacrylate in the polymerization step. See the Supplementary Information for full synthetic procedures and characterization data. Toluene was identified as the best solvent to dissolve BMP, CuBr, PMDETA, MPC, and fluorescein *O*-methacrylate for polymerization reactions. As the reaction progresses, the solubility of the growing chain intermediates change and lessen over time, ultimately affecting the molecular weight distribution of the polymer. Synthesis conditions were optimized to minimise these solubility constraints.

Self-Assembly of 1 and 1′ on Ad-Functionalized Surfaces

Polymer **1** was adsorbed on the **Ti-Ad** or **Glass-Ad** substrates by immersing in a 10 mg/mL aqueous solution of **1** for 12 h. The substrate was then rinsed with deionized water to remove any unconjugated **1** and then allowed to dry under ambient conditions. Surfaces were coated with **1′** by the same method.

Preparation of PMPC-coated AFM Tips

PMPC-coated polystyrene microspheres were prepared by the grafting polymerization initiated by *tert*-butyl hydroperoxide (TBHP) from the amino group of amine-modified polystyrene microspheres (diameter: 4.0–4.9 μm). The PMPC-coated polystyrene microspheres were glued to the end of a tipless AFM cantilever using ultraviolet curing adhesive. The specific experimental operations are described in detail in Supplementary Information.

Competing Interests Statement

The authors declare no competing interests.

Acknowledgements

References

1. Seror, J., Zhu, L., Goldberg, R., Day, A. J. and Klein, J. Supramolecular synergy in the boundary lubrication of synovial joints. (2015) *Nature Commun.* **6**, 6497.

2. Lee, S. and Spencer, N. D. (2008) Sweet, hairy, soft, and slippery. *Science*, **319**, 575–576.

3. Klein, J. Hydration lubrication. (2013) *Friction* **1**, 1–23.

4. Ma, L., Gaisinskaya-Kipnis, A., Kampf, N. and Klein, J. Origins of hydration lubrication. (2015) *Nature Commun.* **6**, 7060.

5. Jahn, S., Seror, J. and Klein, J. Lubrication of articular cartilage. (2016) *Annu. Rev. Biomed. Eng.* **18**, 235–258.

6. Maeda, N., Nianhuan, C., Tirrell, M. and Israelachvilli, J. N. Adhesion and friction mechanisms of polymer-on-polymer surfaces. (2002) *Science* **297**, 379–382.

7. Peng, Y., Wang, Z. and Li, C. Study of nanotribological properties of multilayer graphene by calibrated atomic force

microscopy. (2014) *Nanotechnology* **25**, 305701.

8. Yang, H.K., Khadem, M., Penkov, O. V. and Kim, D.-E. Increased elasticity and damping capacity of diamond-like carbon coatings by immobilized C_{60} fullerene clusters. (2019) *Nanoscale* **11**, 2863–2870.

9. Tambe, N. S. and Bhushan, B. Identifying materials with low friction and adhesion for nanotechnology applications. (2005) *Appl. Phys. Lett.* **86**, 061906.

10. Moro, T. et al. Surface grafting of artificial joints with a biocompatible polymer for preventing periprosthetic osteolysis. (2004) *Nature Mater.* **3**, 829–836.

11. Klein, J. Repair or replacement—a joint perspective. (2009) *Science* **323**, 47–48.

12. Ishihara, K. Highly lubricated polymer interfaces for advanced artificial hip joints through biomimetic design. (2015) *Polym. J.* **47**, 585–597.

13. Martin, H. J., Schulz, K. H., Bumgardner, J. D., Walters, K. B. XPS study on the use of 3-aminopropyltriethoxysilane to bond chitosan to a titanium surface. (2007) *Langmuir* **23**, 6645–6651.

14. Sorkin, R., Kampf, N., Zhuab, L. and Klein, J. Hydration lubrication and shear-induced self-healing of lipid bilayer boundary lubricants in phosphatidylcholine dispersions. (2016) *Soft Matter* **12**, 2773–2784.

15. Zhulina, E. B. and Rubinstein, M. Lubrication by polyelectrolyte brushes. (2014) *Macromolecules* **47**, 5825–5838.

16. Yu, Y. et al. Multivalent counterions diminish the lubricity of polyelectrolyte brushes. (2018) *Science*, **360**, 1434–1438.

17. Raviv, U. et al. Lubrication by charged polymers. (2003) *Nature* **425**, 163–165.

18. Li, J., Ueda, E., Paulssen, D., and Levkin, P. A. Slippery lubricant-infused surfaces: properties and emerging applications. (2019) *Adv. Funct. Mater.* **29**, 1802317.

19. Chen, S., Zhang, N., Zhang, B., Zhang, B. and Song, J. Multifunctional self-healing ionogels from supramolecular assembly: Smart conductive and remarkable lubricating materials. (2018) *ACS Appl. Mater. Interfaces* **10**, 44706−44715.

20. Li, H., Cui, Y., Li, Z., Zhu, Y. and Wang, H. Fabrication of microcapsules containing dual-functional tung oil and properties suitable for self-healing and self-lubricating coatings. (2018) *Prog. Org. Coat.* **115**, 164–171.

21. Morgese, G., Cavalli, E., Müller, M., Zenobi-Wong, M. and Benetti, E. M. Nanoassemblies of tissue-reactive, polyoxazoline graft-copolymers restore the lubrication properties of degraded cartilage. (2017) *ACS Nano*, **11**, 2794−2804.

22. Irie, T. and Uekama, K. Pharmaceutical applications of cyclodextrins. III. Toxicological issues and safety evaluation. (1997) *J. Pharm. Sci.* **86**, 147–162.

23. Chiba, J., Sakai, A., Yamada, S., Fujimotob, K. and Inouye, M. A supramolecular DNA self-assembly based on β-cyclodextrin–adamantane complexation as a bioorthogonal sticky end motif. (2013) *Chem. Commun.* **49**, 6454–6456.

24. Rekharsky, M. V. and Inoue, Y. Complexation thermodynamics of cyclodextrins. (1998) *Chem. Rev.* **98**, 1875–1917.

25. Crini, G. Review: A history of cyclodextrins. (2014) *Chem. Rev.* **114**, 10940–10975.

26. Liu, Z., Nalluri, S. K. M. and Stoddart, J. F. Surveying macrocyclic chemistry: from flexible crown ethers to rigid cyclophanes. (2017) *Chem. Soc. Rev.* **46**, 2459–2478.

27. Harada, A. Takashima, Y. and Nakahata, M. Supramolecular polymeric materials via cyclodextrin−guest interactions. (2014) *Acc. Chem. Res.* **47**, 2128–2140.

28. Yang, X. et al. Self-healing polymer materials constructed by macrocycle-based host–guest interactions. (2015) *Soft Matter* **11**, 1242–1252.

29. Dai, X. et al. A mechanically strong, highly stable, thermoplastic, and self-healable supramolecular polymer hydrogel. (2015) *Adv. Mater.* **27**, 3566–3571.

30. Chen, H., Ma, X., Wu, S. and Tian, H. A rapidly self-healing supramolecular polymer hydrogel with photostimulated room-temperature phosphorescence responsiveness. (2014) *Angew. Chem. Int. Ed.* **53**, 14149–14152.

31. Highley, C. B., Rodell, C. B. and Burdick, J. A. Direct 3D printing of shear-thinning hydrogels into self-healing hydrogels. (2015) *Adv. Mater.* **27**, 5075–5079.

32. de Jong, M. R., Huskens, J. and Reinhoudt, D. N. Influencing the binding selectivity of self-assembled cyclodextrin monolayers on gold through their architecture. (2001) *Chem.—Eur. J.* **7**, 4164–4170.

33. Mulder, A. et al. Molecular printboards on silicon oxide: Lithographic patterning of cyclodextrin monolayers with multivalent, fluorescent guest molecules. (2005) *Small* **1**, 242–253.

34. Xu, R., Ma, S., Wu, Y., Zhou, F. and Liu, W. Promoting lubricity and antifouling properties by supramolecular-recognition-based surface grafting. (2018) *Langmuir* **34**, 13116−13122.

35. Crespo-Biel, O. et al. Multivalent host–guest interactions between β-cyclodextrin self-assembled monolayers and poly(isobutene-*alt*-maleic acid)s modified with hydrophobic guest moieties. (2005) *Chem —Eur. J.* **11**, 2426–2432.

36. Samanta, A. et al. Fabrication of hydrophilic polymer nanocontainers by use of supramolecular templates. (2015) *J. Am. Chem. Soc.* **137**, 1967–1971.

37. Prestch, E. Bühlmann, P. and Badertscher, M. *Structure Determination of Organic Compounds*. (Springer-Verlag, Berlin Heidelberg, 2009).

38. Moulder, J. F., Stickle, W. F., Sobol, P. E. and Bomben, K. D. *Handbook of X-ray Photoelectron Spectroscopy.* (Perkin-Elmer Corp., Eden Prairie, MN, 1992).

39. Blass, J., et al. Switching adhesion and friction by light using photosensitive guest–host interactions. (2015) *Chem. Commun.* **51**, 1830–1833.

40. Blass, J., Albrecht, M., Bozna, B. L., Wenz, G. and Bennewitz, R. Dynamic effects in friction and adhesion through cooperative rupture and formation of supramolecular bonds. (2015) *Nanoscale* **7**, 7674–7681.

41. Guerra, R., Benassi, A., Vanossi, A., Maef, M. and Urbakh, M. Friction and adhesion mediated by supramolecular host–guest complexes. (2016) *Phys. Chem. Chem. Phys.* **18**, 9248–9254.

42. Wang, Y., Sun, Y., Gu, Y. and Zhang, H. Articular cartilage-inspired surface functionalization for enhanced lubrication. (2019) *Adv. Mater. Interfaces* 1900180.

43. Vafaeian, B. et al. Hip joint contact pressure distribution during Pavlik harness treatment of an infant hip: A patient-specific finite element model. (2018) *J. Biomech. Eng.* **140**, 071009.

44. Kyomoto, M. et al. Poly(2-methacryloyloxyethyl phosphorylcholine) grafting and vitamin E blending for high wear resistance and oxidative stability of orthopedic bearings. (2014) *Biomaterials* **35**, 6677–6686.

45. Shihori, Y. et al. Wear resistance of poly(2-methacryloyloxyethyl phosphorylcholine)-grafted carbon fiber reinforced poly(ether ether ketone) liners against metal and ceramic femoral heads. (2018) *J. Biomedical Materials Research B: Applied Biomaterials.* **106B,** 1028−1037.

46. Seido, Y. et al. Influences of dehydration and rehydration on the lubrication properties of phospholipid polymer-grafted cross-linked polyethylene. (2015) *J. Engineering in Medicine.* **229**, 506–514.

47. Napolitano, S. and Wübbenhorst, M. The lifetime of the deviations from bulk behaviour in polymers confined at the nanoscale. (2011) *Nature Commun.* **2**, 260.

48. Fennimore, A. M. et al. Rotational actuators based on carbon nanotubes. (2003) *Nature* **424**, 408–410.

49. Holmberg, K. and Erdemir, A. Influence of tribology on global energy consumption, costs and emissions. (2017) *Friction* **5**, 263–284.

50. Perl, A. et al. Gradient-driven motion of multivalent ligand molecules along a surface functionalized with multiple receptors. (2011) *Nature Chem.* **3**, 317–322.

51. Green, C. P. et al. Normal and torsional spring constants of atomic force microscope cantilevers. (2004) *Rev. Sci. Instrum.* **75**, 1988−1996.

52. Li, J. et al. AFM studies on liquid superlubricity between silica surfaces achieved with surfactant micelles. (2016) *Langmuir* **32**, 5593−5599.

53. Varenberg, M. Etsion, I. and Halperin, G. (2003) An improved wedge calibration method for lateral force in atomic force microscopy. *Rev. Sci. Instrum.* **74**, 3362−3367.

54. Vafaeian, B., et al. Hip joint contact pressure distribution during Pavlik harness treatment of an infant hip: A patient-specific finite element model. (2018) *J. Biomech. Eng.* **140**, 071009.